Individual neurophysiological signatures of spontaneous rhythm processing

A. Criscuolo*, M. Schwartze*, M.J. Henry°, C. Obermeier'[§] & S.A. Kotz*' ^

* Department of Neuropsychology & Psychopharmacology, Faculty of Psychology and Neuroscience, Maastricht University, 6200 MD, Maastricht, the Netherlands

° Max Planck Institute for Empirical Aesthetics, Frankfurt am Main, Germany

[§] BG Klinikum Bergmannstrost Halle, 06112 Halle, Germany

' Department of Neuropsychology, Max Planck Institute for Human Cognitive and Brain Sciences, 04103, Leipzig, Germany

^ Corresponding author

Email: sonja.kotz@maastrichtuniversity.nl

Conflict of interest: none to declare.

Acknowledgements: We thank Ina Koch at the Max Planck for Human Cognitive and Brain Science, Dept. of Neuropsychology, Leipzig, Germany for her support in data collection.

Abstract

When sensory input conveys rhythmic regularity, we are able to form predictions about the timing of upcoming events. Although rhythm processing capacities can differ considerably between individuals, these differences are often obscured by subject- and trial-level data averaging procedures in M/EEG research. Here, instead, we systematically assessed the neurophysiological variability exhibited by individuals listening to isochronous equitone sequences interspersed with unexpected deviant tones. First, we focused on rhythm tracking and tested the phase-relationship between neural activity in the delta-band and pre-tone onsets. We observed clear between- and within-subject variability, confirming that individuals employ variable, flexible, but consistent rhythm tracking at the single-trial level. Next, we modelled single-trial time-locked neural responses in the beta-band to investigate individual tendencies to employ binary or triplet grouping ("tic-toc effect"). Beta-band activity showed binary (strong-weak), triplet (strong-weak-weak) and mixed accentuation patterns, resembling the superimposition of a beat. Thus, we identified individual preferences for grouping patterns and tendencies to switch between binary, triplet, or combined patterns over trials. Notably, we demonstrated that the processing of standard and deviant tones was modulated by the employed grouping.

This approach to neurophysiological profiling offers a sensitive strategy to identify individual and dynamically evolving neural signatures of rhythm and beat processing. We suggest that the observed neurophysiological variability reflects *flexible windows of opportunity* for evaluating and adapting to (un)predictable environmental rhythms.

Significance statement

For decades, music, speech and rhythm research has investigated how humans process, predict, and adapt to environmental rhythms. By taking an individual-trial and -subject approach, we avert the common pooling of EEG data in favor of individual and time-varying neural signatures of rhythm tracking and beat processing. Notably, the superimposition of a beat induces pattern accentuations that affect how individuals respond to expected (standard) and unexpected (deviant) auditory events at the single-trial level. This subject- and trial-based approach supports

individual neural profiling and potentially aids the identification of altered neural activity and its consequences for natural listening.

Introduction

Due to the inherently rhythmic nature of many environmental stimuli, neurocognitive functions such as attention (Lakatos et al., 2008) sensorimotor behavior (Merker et al., 2009), speech (Giraud & Poeppel, 2012), reading (Goswami, 2011), and music (Doelling & Poeppel, 2015) processing rely on basic timing capacities. To generate a temporally coherent representation of the rhythmic environment, we track stimulus periodicities, use smart grouping, and continuously segment and combine multiple inputs in time (Buzsáki, 2009; Large & Jones, 1999; Schroeder & Lakatos, 2009; Thut et al., 2012a; Zoefel & VanRullen, 2016). Dynamic attending theory (Large & Jones, 1999) proposed that timing capacities might reflect how internal rhythms (i.e., neural oscillatory activity) synchronize with external rhythms. This suggests that oscillatory activity instantiates a realistic computational model for "adaptation by anticipation" (Fraisse, 1963; p. 18). Accordingly, temporally regular sensory input would allow that future events are temporally predictable, and thereby facilitate sensory processing, perception, allocation of attention and the overall effectiveness of behavior (Arnal, 2012; Friston, 2005; Háden et al., 2015; Koelsch et al., 2019; Nobre et al., 2012; Schröger et al., 2015).

However, *continuous change is a fundamental characteristic of life* (Schwartze et al., 2011), and we frequently experience irregular rhythms or sudden changes in the environment. Thus, any realistic adaptation likely tolerates a certain degree of temporal irregularity or unpredictability while achieving synchronization (Barnes & Jones, 2000). Hence, endogenous oscillatory activity must not only be precise and stable over time, but also flexible enough to achieve adequate adaptive timing (e.g., speeding-up or slowing-down). As a result, oscillatory brain activity can actively track and process (a)periodic and (un)predictable stimuli such as speech rhythms at phoneme (25-35Hz) to syllable (4-8Hz) and word (1-3Hz) rates (Giraud & Poeppel, 2012) and rapidly adapt to changes in the sensory environment, likely through phase resetting (Barnes & Jones, 2000; Haegens & Zion Golumbic, 2018; Mormann et al., 2005; Obleser et al., 2012a; Zoefel et al., 2018).

Neural oscillatory dynamics in the beta (β; 12-25Hz) and delta (δ; 1-4Hz) frequency range have been associated with rhythm processing, temporal prediction, and attention (Arnal, 2012; Biau & Kotz, 2018; Colling et al., 2017; Fujioka et al., 2012, 2015; Morillon et al., 2016; Nozaradan et al., 2015, 2017a) and in non-human primates (Bartolo & Merchant, 2015; Merchant et al., 2015; Merchant & Bartolo, 2018; Patel & Iversen, 2014). However, the critical question of which

neurophysiological signatures indicate how exactly individuals process the beat and rhythm has so far not been answered. Although prior behavioural studies have demonstrated individual grouping preferences and within-subject variability across trials (Baath, 2015; Poudrier, 2020), the neural counterparts of such variability are still unknown (Waschke et al., 2021). We therefore investigated cortical rhythm tracking, and the human disposition to group two or three adjacent tones when listening to isochronous equitone sequences (Brochard et al., 2003). This mechanism drives binary (strong-weak (S-w)) or triplet (S-w-w) accentuation patterns, resembling the superimposition of a beat. Even with physically identical stimuli, this beat can influence observable behaviour and underlying neural activity (Abecasis et al., 2005; Baath, 2015; Brochard et al., 2003; Poudrier, 2020; Schmidt-Kassow et al., 2011).

Here, participants passively listened to isochronous (1.5Hz) equitone sequences, comprising frequent standard and either one or two amplitude-attenuated deviant tones while their EEG was recorded. We used single-trial phase-locking analyses to quantify how brain activity would predictively align with stimulus rhythms and respond to sudden changes in the environment (i.e., deviant tones). By zooming into single-subject and -trial level delta-band (1.5Hz) dynamics, we reveal flexible but consistent rhythm tracking preceding tone onsets. We then modelled single-subject and single-trial time-locked fluctuations in the beta-band to probe individual differences in beat processing. Neurophysiological data reveal accentuation patterns, with spontaneous tendencies to group auditory input. Hence, we characterize inter- and within-subject predispositions to process a beat, and tendencies to switch between binary, triplet, and combined grouping over time.

The observed neurophysiological variability might provide *flexible windows of opportunity* for evaluating and adapting to (un)predictable environmental rhythms. We suggest that zooming into individual and single-trial neurophysiological variability might meaningfully predict behavioral variability while processing simple and complex environmental rhythms (e.g. speech tracking), in neurotypical and altered cognition.

Materials & Methods

Participants

Twenty native German speakers participated in the study and signed written informed consent in

accordance with the guidelines of the Ethics committee of the University of Leipzig and the Declaration of Helsinki. Participants (9 females; 21-29 years of age, mean 26.2 years) were right-handed (mean laterality coefficient 93.8**,** Oldfield, 1971), had normal or corrected-to-normal vision, no known hearing deficits. Participants received 8€/hr for taking part in the study.

Experimental design and procedure

The stimuli comprised 96 sequences of 13-to-16 400-Hz, 50-ms, 70-dB SPL tones (standard; STD), presented in two recording sessions. One or two deviant tones (DEV), attenuated by 4 dB relative to the STD tones, was embedded in each tone sequence replacing STD tones. The first DEV tone could either occur in an odd or even-numbered position (8-11th), while the second always fell on the 12th position (Fig.1; corresponding to hypothetical binary Strong-weak pattern; S-w). The inter-onset-interval between two successive tones was 650ms, resulting in a stimulation frequency of 1.54Hz for each equitone sequence. Stimuli were thus comparable to those used in previous EEG studies on individual grouping [35,37].

Participants were seated in a dimly lit soundproof chamber facing a computer screen. A trial started with a fixation cross (500ms), followed by the presentation of the tone sequence. The cross was continuously displayed on the screen while tone sequences were played to prevent excessive eye movements. Immediately at end of the tone sequence, a response screen appeared and prompted participants to press a response button to indicate whether they heard one or two softer tones. Button presses were counterbalanced across participants. The inter-trial interval was 2000ms. A session was divided into two blocks of approximately 10 minutes each, with a short pause in between. Therefore, an experimental session lasted for about 25 minutes.

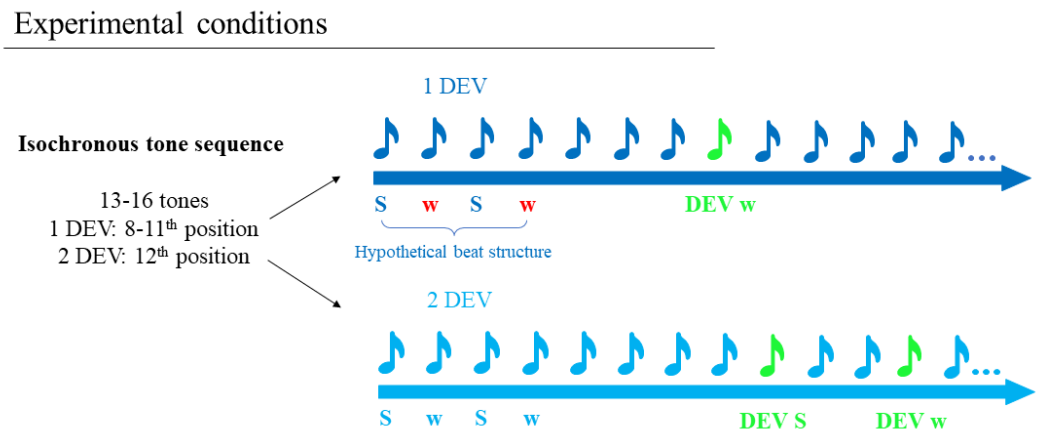

Figure 1 - Experimental conditions.
Participants listened to 96 isochronous tone sequences, containing 13-to-16 tones and either one or two deviants (DEV). The first DEV could either fall on positions 8,9,10,11th, while the second DEV always fell on position 12th. A hypothetical binary grouping structure could segment adjacent tones as Strong-weak (S-w; or on-/off-beat) tones. Thus, the first DEV could occur with equal probability in S-w tone positions.

EEG recording

The EEG was recorded from 59 Ag/AgCl scalp electrodes (Electrocap International), amplified using a PORTI-32/MREFA amplifier (DC to 135 Hz), and digitized at 500 Hz. Electrode impedances were kept below 5kΩ. The left mastoid served as online reference. Additional vertical and horizontal electro-oculograms (EOGs) were recorded.

Data Analysis

Preprocessing

Data were pre-processed using combined custom Matlab scripts/functions and the Matlab-based FieldTrip toolbox [41]. Data were re-referenced to the average of the two mastoid electrodes, band-pass filtered with a 4th order Butterworth filter in the frequency range of 0.5-50 Hz (*ft_preprocessing*). Eye-blinks and other artifacts were identified using independent component analysis ('*fastICA'* implemented in FieldTrip). A semi-automated pipeline was used to identify EEG components with a strong correlation (>.4) with the EOG time-courses, to inspect the respective topographical distribution across scalp electrodes, and to remove "bad" components. Next, data segmentation was either trial-locked in the rhythm-tracking analyses or event-locked for event-related potential [ERP] and time-frequency representation [TFR] analyses.

Rhythm tracking analyses

Trial-locked analyses covered the whole auditory sequence. Following ICA, we created 192 (96 auditory sequences * 2 sessions per subject) 11s-long segments starting from the third tone onset up to the 13th tone. Next, we created a bilaterally distributed fronto-central channel cluster average, encompassing the sensor-level correspondents of prefrontal, pre-, para-, and post-central regions highlighted in previous studies (Fujioka et al., 2012; Fujioka et al., 2015). A fronto-central cluster included the following 16 channels: 'AFz', 'AF3', 'AF4', 'F3', 'F4', 'F5', 'F6', 'FCz', 'FC3', 'FC4', 'FC5', 'FC6', 'C1', 'C2', 'C3', 'C4'. Data from this fronto-central cluster were used for Fast-Fourier transform (FFT) and phase-locking analyses.

Fast-Fourier transform

Single-trial data averaged across electrodes in the fronto-central cluster were submitted to a FFT (referred to as FFT data) with an output frequency resolution of 0.14Hz. Spectral power was calculated as the squared absolute value of the complex Fourier output. Data in each frequency bin were normalized by the frequency-specific standard deviation across trials. We then subtracted from each data point the mean across 4 neighboring frequency bins on either side (frequency-band for the averaging: 0.14Hz*4 on either side; (Nozaradan et al., 2017b)). Lastly, we averaged the data across trials. For illustration purposes, we restricted the Fourier spectrum from 1-to-4Hz (Fig. 2A).

Phase-locking analyses

A time-resolved phase-locking analysis was performed to estimate the phase relationship between neural activity at the stimulation frequency and the sequential tone onsets. We also tested whether unpredictable events (i.e., a DEV) would alter the phase relationship between neural activity and stimulus onsets. Timely changes in phase locking might resemble reactive adaptation in response to sudden environmental changes, instantiated in phase reset of oscillatory activity (Barnes & Jones, 2000; Zoefel et al., 2018).

Trial-level data from the fronto-central cluster average were bandpass-filtered around the stimulation frequency (1.04-2.04Hz, to obtain a 1.54Hz center frequency; *ft_preprocessing*) and Hilbert-transformed to extract the analytic signal. Next, we plotted the time-course of the absolute values of the analytic signal (Fig.3B) as a function of the STD tone onsets preceding

(blue) and following (red) the DEV (green) for illustrative purposes only. Phase-locking analyses were performed by means of circular statistics and based on the circular mean phase-angles estimated in the ~60ms (1/1.54Hz/10) preceding individual tone onsets. Next, phase angles were plotted with polar histograms for STD tones preceding (blue; from the third onwards) and following (red) the onset of a DEV tone (Fig.3C). The phase-angle circular difference in the between pre- and post-DEV positions was assessed at the single-subject level by means of 1000 permutations of pre-/post-DEV labels. A p-value lower than .05 was considered statistically significant. Lastly, we calculated the trial-based mean vector length (MVL) for pre-DEV tones and statistically assessed it against the MVL from a random distribution (random phase-angles) by means of 1000 permutation tests. A p-value lower than .05 was considered statistically significant.

ERP and TFR data

After ICA, data were segmented into 4s-long epochs symmetrically time-locked to every tone onset. Next, we employed an automatic channel-by-channel and epoch-by-epoch single-subject artifact suppression procedure. Amplitude values were temporarily normalized by their standard deviation across trials and outliers (data points per epoch and channel) were defined by means of a threshold criterion (values > mean + 2*SD). The identified noisy time-windows (with 50ms symmetrical padding) then served to suppress (replace by NaNs) time-points in the non-normalized data and these missing values were replaced by means of cubic temporal interpolation (*'pchip'* option for both the built-in Matlab and FieldTrip-based interpolation functions) with neighboring time-windows (700ms when possible, automatically reduced otherwise). Thus, rather than rejecting entire epochs containing artifacts (i.e., standard artifact rejection procedure), we opted for an artifact suppression approach which kept all trials. Note that the channel-by-channel routine allowed the algorithm to flexibly adapt the outlier threshold estimates to the inherent noise varying over channels. Lastly, a standard whole-trial rejection procedure based on amplitude criterion (85uV) was also applied. Data destined for event-related-potential (ERP) analyses ("ERP data") were segmented including 500ms prior and following each tone onset (1s in total). Data destined to time-frequency representation analyses ("TFR data") were not further segmented at this stage. ERP data were band-pass filtered between 1-30Hz and TFR data low-pass filtered at 40Hz. Data were then downsampled to 250Hz.

TFR data finally underwent time-frequency transformation by means of a wavelet-transform [44], with a frequency resolution of .25Hz. The number of fitted cycles ranged (gradually) from 3 for the low frequencies (<5Hz) to 10 for high frequencies (>5Hz and up to 40Hz). TFR data were then re-segmented to reduce the total length to 2s, symmetrically distributed relative to tone onsets.

Post-processing of ERP and TFR data

Single-trial ERP amplitudes were mean-corrected by a global average over all epochs and 500ms long (-0.2 to 0.3s relative to tone onset). Similarly, single-trial TFR amplitudes were normalized by computing relative percent change with reference to the global mean amplitude across epochs and 500ms long (-0.2 to 0.3s relative to tone onset). This previously applied approach (Abbasi & Gross, 2020; Fujioka et al., 2012) was preferred over classical baseline correction because we aimed at analyzing amplitude fluctuations in the pre-stimulus intervals. Finally, we calculated a fronto-central channel cluster average (as above). All subsequent analyses were performed exclusively on this channel cluster.

ERP analyses

We averaged evoked responses over trials separately for STD and DEV tones, and for odd (hypothetical "Strong" position in a binary beat; S, Fig. 1) and even ("weak"; w) serial positions from the 3rd to the 11th tone. The first two positions were not included to exclude the increased responses typically observed at the beginning of an auditory sequence. Fig. 2G–H shows the respective ERPs for the averaged fronto-central channel, for STD tones on metrically strong and weak positions (Fig. 2G) and for the comparison of STD and DEV tones averaged over metric positions (Fig. 2H). Statistical analysis was performed by means of paired-sample t-tests. An adjusted p-value lower than .05 was considered statistically significant (Benjamini & Hochberg correction).

TFR analyses

We averaged time–frequency representations over STD trials, separately for odd and even positions (hypothetical strong and weak positions, respectively; Fig. 2E). Next, we quantified mean amplitudes in the low-beta band (low-β; 12-20Hz) in the pre- and post-stimulus intervals

(150ms before and after stimulus onset, respectively) and compared them for S-w positions (Fig. 2E).

Single-subject beat classification

We investigated individual beat processing differences by employing a modelling approach suited to reveal binary, triplet, and other potential forms of grouping. We focused on single-subject, low-β peak amplitudes for STD tones in the first 8 positions of the auditory sequence in two time-windows time-locked to the stimulus onset, one preceding (labeled as 'β-pre') and one following (labeled as 'β-post') stimulus onset. Within these time-windows, we extracted mean peak amplitudes from a time-window, whose length was proportional to the center frequency of interest (for low-β: 1/16Hz = 60ms).

Single-tone β-post amplitudes were first concatenated to mimic an 8-tone auditory sequence (i.e., a trial). Single-subject and trial-level β-post amplitude fluctuations (8 tones) were then entered into a stepwise regression model (Fig. 3A) ('*stepwiselm*' in Matlab) with 3 predictors: binary (values: 1, -1), triplet (1, -.5, -.5), and a constant term (ones). The winning model was chosen based on adjusted Eta-squared. Trials for which the winning model involved the binary predictor were labeled "binary", whether the winning model included the intercept term. Similarly, trials for which the winning model involved the triplet predictor were labeled "triplet" independent of whether the intercept was included in the mode. The model thus allowed combination of multiple predictors, but no interactions between terms. We accordingly interpreted (and labeled) the combination of binary and triplet terms as "combined predictor". Lastly, trials in which grouping could not be clearly identified were labeled as "not classified".

Binary group analyses

We vertically concatenated trials classified as "binary" (Fig. 3C) and then computed a trial-based single-tone pair-wise amplitude difference (its lower-triangle 2-D mean is provided in Fig. 3D). In other words, for each trial we calculated the difference between responses to every tone (1-8 positions) along the auditory sequence. Thus, the amplitude for the 1st position was compared to the 2nd, then to the third position, and so forth. In turn, the amplitude on the 2nd position was compared to the 3rd, the 4th position, and so forth. The resulting pair-wise amplitude difference matrix had a size of N trials x N positions-1. From this matrix we derived two variables, "binary

similarity" and "binary dissimilarity". The first denotes the mean difference for tones in hypothetical odd positions, averaged together with the mean difference for tones in hypothetical even positions. The second denotes the mean difference of tones in odd versus even positions (Fig. 3E). Statistical testing was performed by means of 1000 permutations of odd-even labels, and an FDR-adjusted p-value lower than .05 was considered statistically significant (Benjamini & Hochberg correction). The same mean extraction and pair-wise amplitude difference procedure was repeated for β-pre (Fig. 3F).

DEV analyses as a function of binary beat

For each participant, we identified binary trials and used them to examine DEV processing. We investigated whether DEV tones would elicit different ERP responses according to their metric (S-w) position in the auditory sequence. We performed statistical analyses by comparing ERPs to DEV tones in even- (8,10th) versus odd-numbered (9,11th) positions. Notably, we considered possible 'pure binary' and 'phase-shifted binary' beats (or inverse binary), where the former grouping corresponds to the typical S-w pattern in odd and even positions, and the second the reverse w-S pattern. If such individual grouping varies in time to develop over a trial, it may start in either odd or even positions. The selection was informed by the beta coefficients associated with the identified binary trials: a positive coefficient would indicate 'pure binary', while a negative coefficient would correspond to the 'inverse binary'. Hence, we re-ordered metrical S-w positions according to individual binary beats (odd-numbered positions fall on S beats in 'pure binary' but on w in 'inverse binary'), and statistically compared their associated ERPs time-courses. Statistical testing was performed by means of paired-sample t-tests, and an FDR-adjusted p-value lower than .05 was considered as statistically significant (Benjamini & Hochberg correction).

Code Accessibility

The code in use for analyzing this dataset has been stored and can be provided upon reasonable request by the corresponding author.

Results

Rhythm tracking

When individuals listen to isochronous equitone sequences, their neural activity reflects the timing of external events (Fig.2A-B). Indeed, the Fourier spectrum showed a clear peak at the stimulation frequency (1.5Hz; Fig. 2A) and the time-course of neural activity showed a tendency to align to tones onsets (Fig. 2B). Phase-locking analyses focused on the ~60ms prior to tone onsets revealed a preferential phase-relationship between ongoing brain activity and STD onsets: the trial-based mean vector lengths (MVL) of pre-DEV phase-angles significantly differed from a random distribution (Fig. 2C, histogram; pre-DEV in blue; Suppl. Tab. 1 for stats). However, subject-level trial-averages of single-tone phase-angles did not show a specific clustering (Fig. 2C, polar plot in blue), and did not differ from a random distribution (Suppl. Tab. 1). Next, we tested whether the occurrence of a DEV tone would alter brain-rhythm coupling for the following STD tones. Phase alignment did not change following the DEV tone (Fig. 2C, in red; Suppl. Tab. 1 for stats).

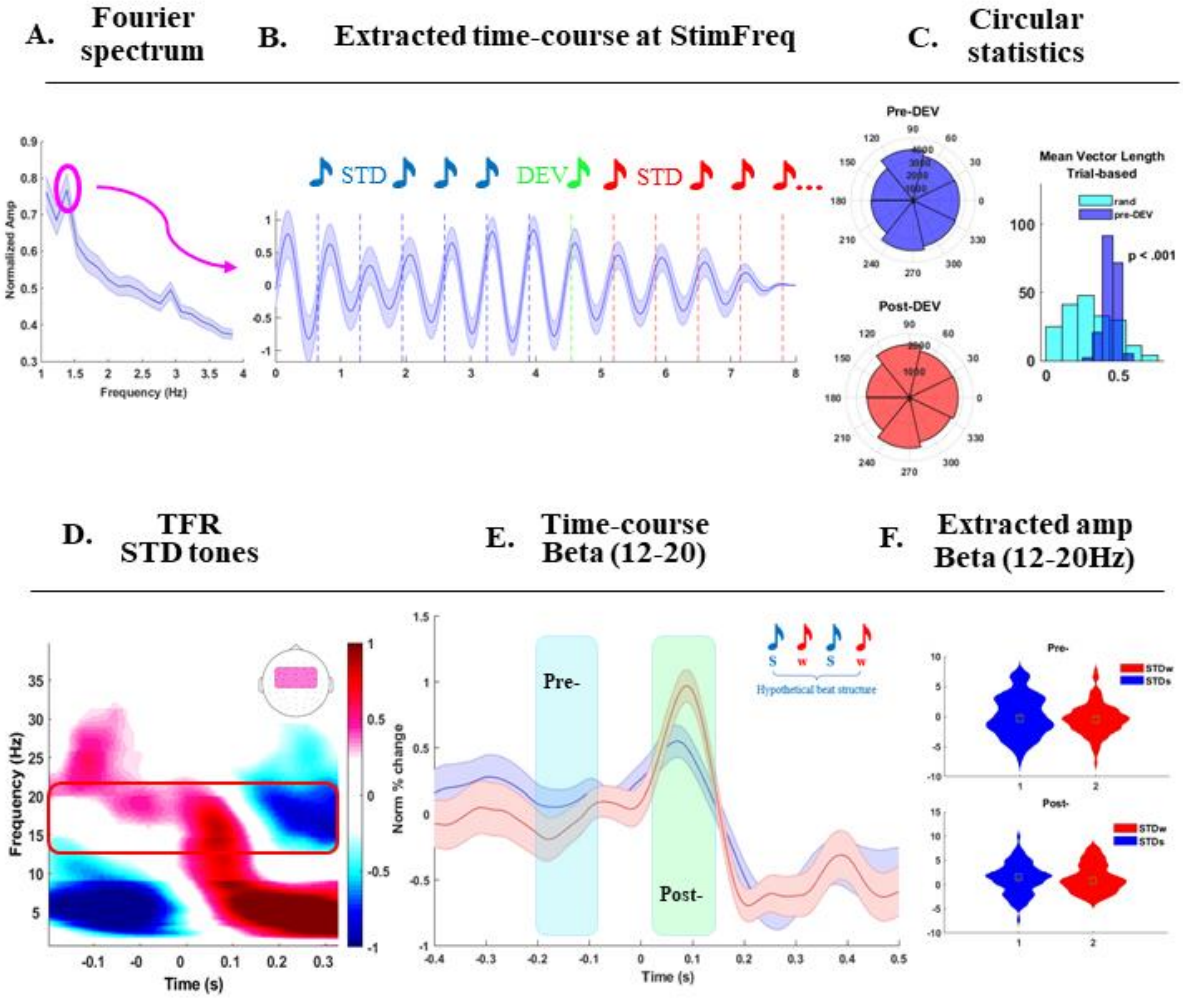

Event-Related Potentials

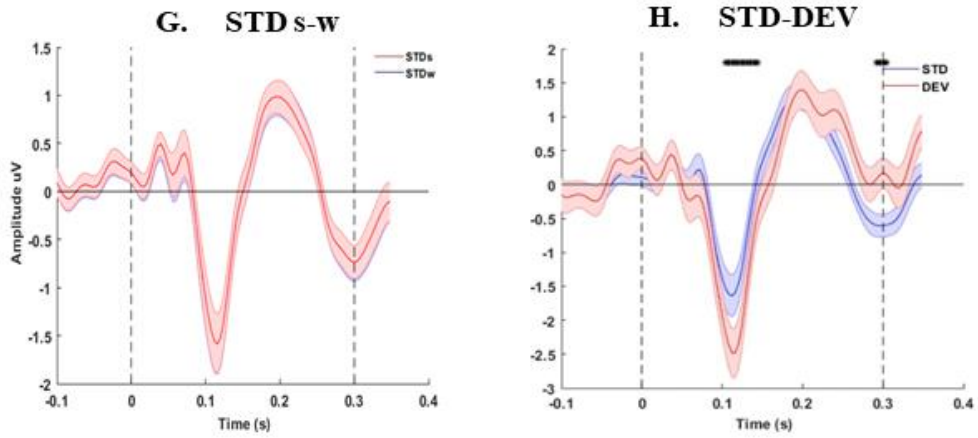

Figure 2 – Rhythm tracking and beat processing.
A: Fourier spectrum of neural activity along the entire auditory sequence. The plot displays the grand-average normalized amplitude in the frequency range from 1 to 4Hz. The pink circle highlights the peak amplitude for neural activity at the stimulation frequency (~1.5Hz). B: time-course of neural activity at the stimulation frequency. Vertical bars indicate the onsets of STD tones prior- (blue) and post-DEV (red). The DEV onset is reported in green. Blue shades represent the standard errors. C: Polar histograms of group-level phase-angles extracted from 60ms prior to the onsets of STD tones prior- (blue) and post-DEV (red). Next to it, the trial-based mean vector length (MVL) for pre-DEV (blue) as compared to the MVL for random distribution of phase-angles. Single-subject statistics are reported in Suppl. Tab. 1. D: grand-average time-frequency spectrum time-locked to STD tones (-.2 to .35s). The frequency range spans from 1-to-40 Hz with a frequency resolution of .25Hz. The red rectangle highlights evoked responses in the low-beta (12-20Hz) frequency range, subject to the following analyses. The topographic plot on top displays the FC cluster average in use. E: extracted time-course of low-beta activity, time-locked to STD tones onsets, in blue for odd-numbered positions (Strong binary grouping) and red for even-numbered positions (weak binary grouping). Shaded colors report standard errors. On top, a blue rectangle delineates the time-window in use for amplitude extraction of low-beta amplitude prior to the STD onset ('pre-'), while the green rectangle is for the time-window after the tone onset ('post-'). F: distribution of low-beta amplitudes extracted from 'pre-' and 'post-' stimulus time-windows highlighted in E, and for STD tones falling on metric binary S (blue) or w (red) positions. G: ERP responses for STD tones on metric S (blue) w (red) positions. H: ERP responses for STD (blue) and DEV tones. Stars indicate significant time-windows, as assessed by means of paired-sample t-tests (FDR-adjusted p <.05).

Beat processing

The power spectrum of neural activity in response to STD tones mainly showed two event-locked responses (Fig. 2D): one in the theta (4-8Hz) and one in the low-beta (low-β; 12-20Hz) frequency-band. Following our hypotheses, we focused on the time-course of activity in the low-β range and compared event-locked amplitude fluctuations for STD tones on odd to even numbered positions along the sequence (Fig. 2E), corresponding to hypothetical S-w binary grouping (blue and red, respectively). Thus, we extracted mean amplitudes in 60ms time-windows (1/16Hz, the center frequency) preceding (labelled as β-pre) and following (β-post) the tone onsets and statistically compared their values for STD tones on hypothetical S-w positions. Statistical testing yielded no significant differences. Similarly, event-related responses (ERPs) to STD tones on S-w positions did not differ (Fig. 2G). However, DEV tones elicited stronger N100 responses as compared to STD tones (FDR-adjusted $p < .05$; Fig. 2H).

Beat modelling

We used a trial-based stepwise regression model to classify single-subject, single-trial beta-band neural responses as best reflecting a binary, triplet, combined, or ambiguous group. The model predicted tone-by-tone low-β-post peak power from three predictors (binary, triple, and constant terms; Fig. 3A). Resulting grouping preferences are reported in Suppl. Tab. 2.

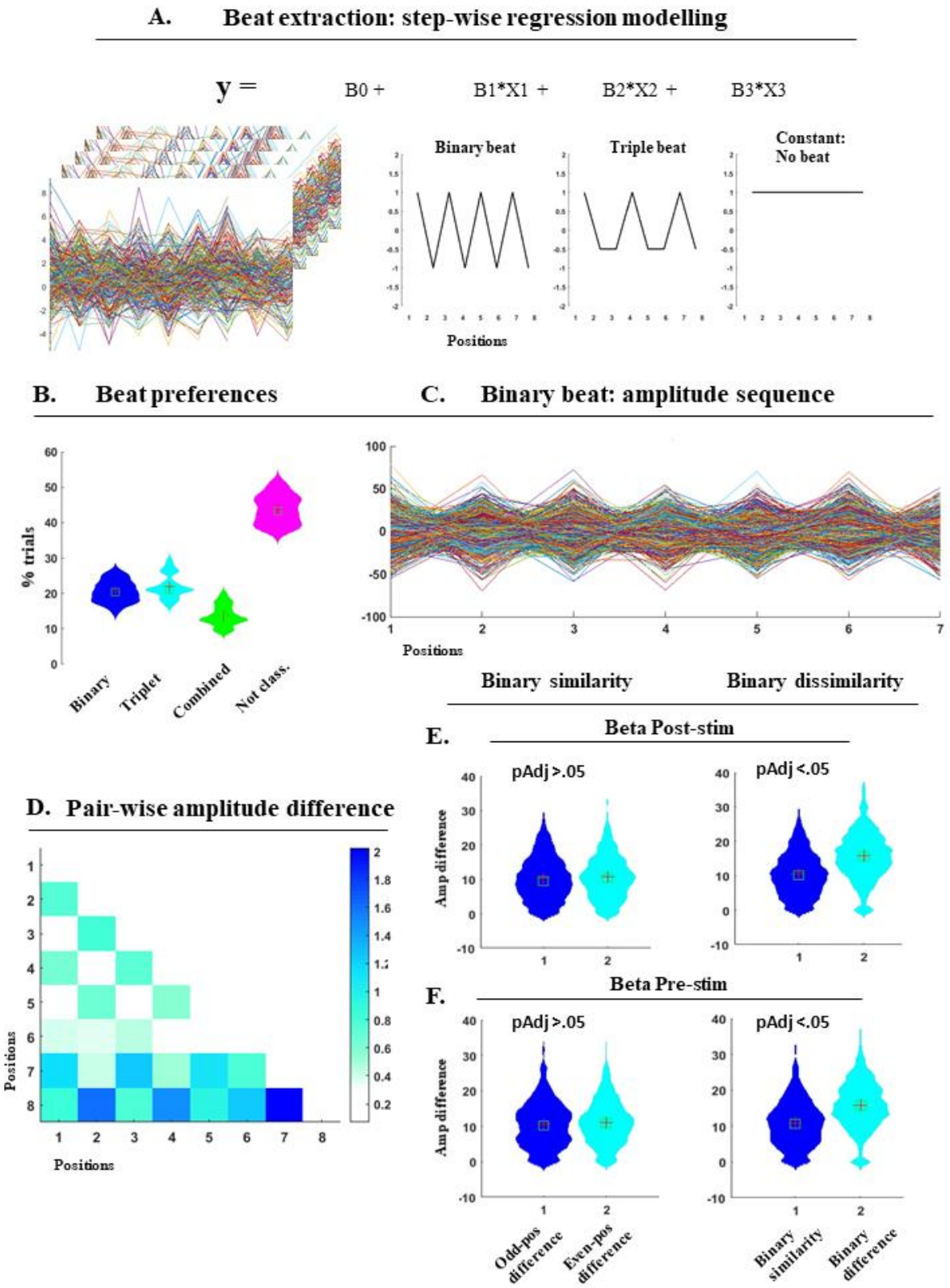
A. Beat extraction: step-wise regression modelling
y = B0 + B1*X1 + B2*X2 + B3*X3
Binary beat
Triple beat
Constant: No beat
Positions
B. Beat preferences
% trials
Binary
Triplet
Combined
Not class.
C. Binary beat: amplitude sequence
Positions
Binary similarity
Binary dissimilarity
D. Pair-wise amplitude difference
Positions
Positions
E. Beta Post-stim
pAdj >.05
pAdj <.05
Amp difference
F. Beta Pre-stim
pAdj >.05
pAdj <.05
Amp difference
Odd-pos difference
Even-pos difference
Binary similarity
Binary difference

Figure 3 – Beat modelling and preferences.
A: Beat modelling was performed by means of stepwise regression modelling and using low-beta evoked responses as a dependent variable. The predictors were a binary (1, -1), a triple (1, -.5, -.5) and a constant term (ones). B: grouping preferences, as reported from the beat modelling. In order, we plot the distribution of trials assigned to binary, triplet, combined (binary-triplet) grouping, and 'not classified' (neither binary nor triplet) across subjects. C: low-beta amplitudes plotted in function of the first 8 positions of the auditory sequence for the binary grouping trials. D: grand-average pair-wise amplitude difference for low-beta peaks across the first 8 positions of the auditory sequence. E, F: on the left, the distribution of amplitude differences across odd-numbered positions (in blue) and even-numbered positions (cyan). The average of these two distributions forms the 'Binary similarity'. On the right, the 'binary similarity' (blue) and the mean amplitude difference of odd- versus even-numbered position ('binary dissimilarity'; in cyan). Statistical testing was performed by means of thousand permutation testing, and an FDR-adjusted p < .05 was considered as statistically significant. Top: for low-beta peak amplitudes post-stimulus. Bottom: low-beta peak amplitudes pre-stimulus.

Binary beat

The identified 'binary beat' trials were vertically concatenated (Fig.3C, for visualization purposes). We then calculated the tone-by-tone pair-wise amplitude difference for low-β post- and pre-STD separately. For visualization purposes, the resulting matrix was averaged across trials and the upper symmetrical triangle was masked (Fig.3D, based on low-β-post). The original matrix (all trials) was used to calculate metrics of "Binary similarity" and "Binary dissimilarity" (Fig.3E, F; top for low-β-post and bottom for low-β-pre). The Binary similarity features two distributions: the amplitude difference for tones in odd-numbered positions (1-3-5-7th; "blue", labeled as "odd-numbered position difference") and the amplitude difference for tones on even-numbered positions (2-4-6-8th; cyan, labeled as "even-numbered position difference"). Statistical testing of these two distributions (odd- and even-numbered position amplitude differences) was not significant. These values were then combined to create a variable labeled as "Binary similarity". For the "Binary dissimilarity" we calculated the amplitude difference for tones on odd- versus even-numbered positions (corresponding to on-beat versus off-beat), which was then labeled as "Binary difference". Thus, the right-side plots in Fig.3E, F feature the Binary similarity versus the Binary difference. Statistical testing yielded a significant difference (FDR-adjusted $p < .05$). The same procedure was repeated, independently, for low-β post- and pre-STD amplitudes.

DEV processing based on binary grouping

We investigated whether DEV tones falling on S-w beat positions would be differentially processed and elicit different ERP responses. Isolating the identified binary trials, we discerned 'pure binary' from 'inverse binary' trials based on the beta-coefficient resulting from the

regression modelling and pooled together odd-numbered (9,11th positions) and even-numbered (8,10th) DEV positions creating grand-averages for 'Odd' and 'Even' positions (i.e., corresponding to S-w). Statistical comparison of the respective ERPs yielded no significant difference in early time-windows but a significant effect in the P3 time-window (p = .02, t = 2.28, CI = 0.1: 1.85; Fig. 4). Indeed, at around 300ms the DEV tones falling on odd-numbered positions produced larger ERP amplitudes than those on even-numbered positions.

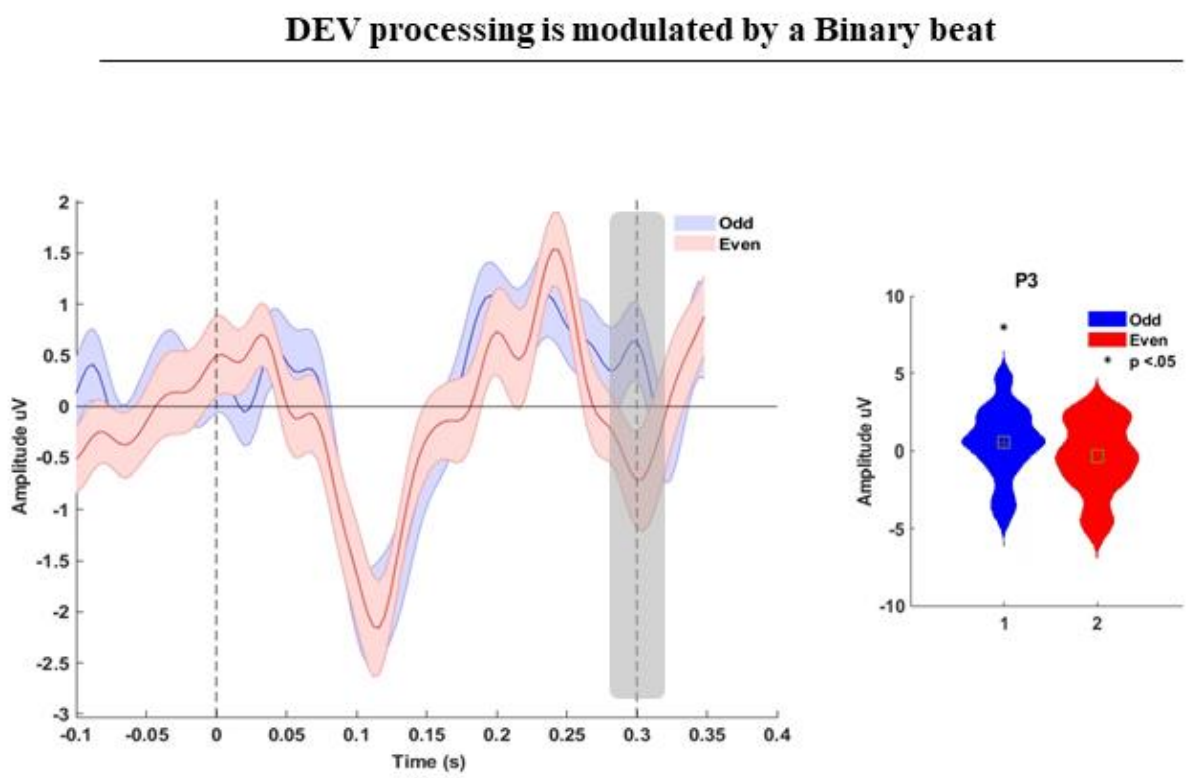

Figure 4 – DEV processing is modulated by a Binary beat.
We statistically compared ERP time-courses (left side) for DEV tones on odd-numbered (blue) versus even-numbered (red) positions in those trials classified as "binary". A significant P3 effect emerged (as highlighted by grey shaded bar). On the right, the extracted P3 amplitude distributions for DEV on odd and even-numbered positions were statistically compared by means of within-subject t-test.

Discussion

The current study aimed at exploring individual neurophysiological variability in rhythm and beat processing. When listening to isochronous equitone sequences, participants' neural activity tracked the timing of external events (Fig.2A), aligning delta-band oscillatory dynamics to tone onsets (Fig.2B-C) (Buzsáki, 2009; Large & Jones, 1999; Schroeder & Lakatos, 2009; Thut et al.,

2012b; Zoefel & VanRullen, 2016). Hence, trial-level mean vector lengths of delta-band activity showed that phase-angles in pre-tone intervals were tightly clustered, confirming active and anticipatory coupling of brain activity to the timing of environmental stimuli. Notably, when pooling trials at the group-level, phase-angles did not differ from random distributions. This suggests that although the brain might generate temporal predictions to achieve successful rhythm tracking (Large & Jones, 1999) to optimize sensory processing, perception, and allocation of attention (Arnal, 2012; Friston, 2005; Háden et al., 2015; Koelsch et al., 2019; Nobre et al., 2012; Schröger et al., 2015), this mechanism may rely on flexible phase-alignment, which tends to vary over time and across individuals, but is consistent within a specific trial.
Next, we tested the effects of an unexpected auditory event. The onset of a deviant tone could either disrupt brain-stimulus coupling or trigger adaptive phase-resets (Barnes & Jones, 2000; Haegens & Zion Golumbic, 2018; Mormann et al., 2005; Obleser et al., 2012b; Zoefel et al., 2018), which re-establish phase-alignment. To address this question, we compared the phase-angles for STD tones before and after a DEV tone (Fig.2C, blue and red respectively) and found no significant differences (Suppl. Tab.1). This result points to the emergence of an adaptive mechanism which enables the system to timely react to changes in the sensory environment, perhaps via mechanisms of phase-reset of oscillatory activity (Barnes & Jones, 2000; Haegens & Zion Golumbic, 2018; Mormann et al., 2005; Obleser et al., 2012b; Zoefel et al., 2018).
After rhythm tracking, we investigated the neural signatures associated with the human disposition to group two or three adjacent tones when listening to isochronous equitone sequences (Brochard et al., 2003). This spontaneous mechanism induces binary (strong-weak (S-w)) or triple (S-w-w) accentuations patterns (Brochard et al., 2003), and might resembles the superimposition of a beat structure. Importantly, while the tones are physically identical, the beat can influence observable behaviour and underlying neural activity (Nozaradan, 2014; Nozaradan et al., 2011, 2016, 2017a; Schmidt-Kassow et al., 2011). So far, however, behavioural and neuroimaging research has dedicated little space to investigations of individual differences. Thus, the question remains whether participants would naturally engage in beat processing and if they would do so in a comparable manner. To address this question, we focused on subject-level neurophysiological variability and modelled single-trial beta-band evoked activity (Fig.3A) to probe whether accentuation patterns mirror binary, triple, and other forms of grouping. Neural activity in the beta-range has been associated with rhythm (Arnal, 2012; Biau & Kotz, 2018;

Fujioka et al., 2012; Fujioka et al., 2015; Morillon et al., 2016) and beat processing (Fujioka et al., 2012; Fujioka et al., 2010). The current findings confirm its prevalence in time-locked responses to STD tones (Fig.2D), corroborated by activity in the theta-band. Furthermore, beta-band activity shows an individuals' spontaneous disposition to process a beat, even when not instructed to do so (Fig.3B). Hence, we characterized inter- and within-subject differences in using binary, triple, and combined grouping over time (Suppl. Tab. 2). Engaging beat processing in absence of specific task instruction might reflect the automatic predisposition to temporally organize continuous auditory input streams in predictable, coherent, and finite units (i.e., beat groups). Thus, the allocation of attentional resources can be discretized (Bolton, 1984; Jones, 1976; Schroeder & Lakatos, 2009) (rather than distributed equally over time), and can vary within each attentional cycle to attribute salience to on-beat events. We tested this view by particularly focusing on binary grouping (Fig.3C) and showed that beta amplitudes for tones falling on odd-numbered (on-beat or 'strong' ('S')) positions were significantly different from those on even-numbered positions (off-beat or 'weak' ('w'); Fig. 3D-F). This effect suggests that individuals superimpose a binary meter (S-w beat) while listening to auditory sequences. Such grouping resembles the active parsing and segmentation of continuous sensory streams and might serve to allocate attentional resources to salient sensory events, to ultimately optimize perception (Nobre & Van Ede, 2018; Shalev et al., 2019). To test this view, we compared neural responses to unpredicted (deviant) tones falling on S-w positions and found a P3 ERP response. This result replicates earlier results (Brochard et al., 2003; Schmidt-Kassow et al., 2011) and indicates that beat processing might affect how we allocate attention to the auditory environment. Indeed, the P3 is an ERP response elicited by unexpected or novel stimuli, associated with an attentional shift to such stimuli (Escera et al., 2000; Sams et al., 1985; Schröger et al., 2000). However, further investigations are needed to clarify this intricate link between attention deployment, attentional shifts, and beat processing in listening contexts.

In summary, we identify individual rhythm tracking and beat processing differences, and associate them with specific delta-band phase-coupling mechanisms and to beta-band amplitude dynamics, respectively. Thus, we showcase the feasibility of using EEG to identify individual neurophysiological signatures of rhythm cognition. We suggest that most common trial- and group-level averaging approaches might inevitably obscure inter-individual differences and trial-by-trial variability. In contrast, the approach adopted here allows the monitoring of

neurophysiological variability that provides *flexible windows of opportunity* for evaluating and adapting to (un)predictable environmental stimuli. Consequently, we propose that zooming into individual variability might allow to better predict behavioral variability in processing simple and complex environmental rhythms (e.g. speech tracking) in neurotypical and pathological populations (Schwartze et al., 2015, 2016).

Conclusions

When listening to isochronous equitone sequences, humans' neural activity tends to spontaneously align and track the timing of auditory events. Moreover, the current results indicate that individuals can endogenously engage in beat processing by accentuating auditory sequences with binary, triplet, and combined beats. We explored inter-individual and trial-level neurophysiological variability in rhythm cognition, and reveal flexible, time-varying neural mechanisms to effectively evaluate and adapt to rhythms of the external environment. The combined findings highlight that an individualized analysis approach to neurophysiological data can indicate meaningful variation in a listening context that should be considered in a more differentiated account of auditory timing.

References

Abbasi, O., & Gross, J. (2020). Beta-band oscillations play an essential role in motor–auditory interactions. *Human Brain Mapping*, *41*(3), 656–665. https://doi.org/10.1002/hbm.24830

Abecasis, D., Brochard, R., Granot, R., & Drake, C. (2005). Differential brain response to metrical accents in isochronous auditory sequences. *Music Perception*. https://doi.org/10.1525/mp.2005.22.3.549

Arnal, L. H. (2012). Predicting "When" Using the Motor System's Beta-Band Oscillations. *Frontiers in Human Neuroscience*, *6*. https://doi.org/10.3389/fnhum.2012.00225

Baath, R. (2015). *SUBJECTIVE RHYTHMIZATION:A REPLICATION AND AN ASSESSMENT OF TWO THEORETICAL EXPLANATIONS*. 244–254.

Barnes, R., & Jones, M. R. (2000). Expectancy, Attention, and Time. *Cognitive Psychology*. https://doi.org/10.1006/cogp.2000.0738

Bartolo, R., & Merchant, H. (2015). β oscillations are linked to the initiation of sensory-cued movement sequences and the internal guidance of regular tapping in the monkey. *Journal of Neuroscience*. https://doi.org/10.1523/JNEUROSCI.4570-14.2015

Biau, E., & Kotz, S. A. (2018). Lower beta: A central coordinator of temporal prediction in multimodal speech. *Frontiers in Human Neuroscience*, *12*(October), 1–12. https://doi.org/10.3389/fnhum.2018.00434

Bolton. (1984). Rhythm. *The American Journal of Psychology*, *6*(2), 1–46.

Brochard, R., Abecasis, D., Potter, D., Ragot, R., & Drake, C. (2003). The "Ticktock" of Our Internal Clock. *Psychological Science*, *14*(4), 362–366. https://doi.org/10.1111/1467-9280.24441

Buzsáki, G. (2009). Rhythms of the Brain. In *Rhythms of the Brain*. https://doi.org/10.1093/acprof:oso/9780195301069.001.0001

Colling, L. J., Noble, H. L., & Goswami, U. (2017). Neural entrainment and sensorimotor synchronization to the beat in children with developmental dyslexia: An EEG study. *Frontiers in Neuroscience*, *11*(JUL). https://doi.org/10.3389/fnins.2017.00360

Doelling, K. B., & Poeppel, D. (2015). Cortical entrainment to music and its modulation by expertise. *Proceedings of the National Academy of Sciences of the United States of America*, *112*(45), E6233–E6242. https://doi.org/10.1073/pnas.1508431112

Escera, C., Alho, K., Schröger, E., & Winkler, I. (2000). Involuntary attention and distractibility

as evaluated with event-related brain potentials. *Audiology & Neuro-Otology*, *5*(3–4), 151–166. https://doi.org/10.1159/000013877

Friston, K. (2005). A theory of cortical responses. *Philosophical Transactions of the Royal Society B: Biological Sciences*. https://doi.org/10.1098/rstb.2005.1622

Fujioka, T., Trainor, L. J., Large, E. W., & Ross, B. (2012). Internalized Timing of Isochronous Sounds Is Represented in Neuromagnetic Beta Oscillations. *Journal of Neuroscience*, *32*(5), 1791–1802. https://doi.org/10.1523/JNEUROSCI.4107-11.2012

Fujioka, Takako, Ross, B., & Trainor, L. J. (2015). Beta-band oscillations represent auditory beat and its metrical hierarchy in perception and imagery. *Journal of Neuroscience*. https://doi.org/10.1523/JNEUROSCI.2397-15.2015

Fujioka, Takako, Trainor, L. J., Large, E. W., & Ross, B. (2012). Internalized timing of isochronous sounds is represented in neuromagnetic beta oscillations. *Journal of Neuroscience*. https://doi.org/10.1523/JNEUROSCI.4107-11.2012

Fujioka, Takako, Zendel, B. R., & Ross, B. (2010). Endogenous Neuromagnetic Activity for Mental Hierarchy of Timing. *Journal of Neuroscience*, *30*(9), 3458–3466. https://doi.org/10.1523/JNEUROSCI.3086-09.2010

Giraud, A. L., & Poeppel, D. (2012). Cortical oscillations and speech processing: Emerging computational principles and operations. *Nature Neuroscience*, *15*(4), 511–517. https://doi.org/10.1038/nn.3063

Goswami, U. (2011). A temporal sampling framework for developmental dyslexia. *Trends in Cognitive Sciences*, *15*(1), 3–10. https://doi.org/10.1016/j.tics.2010.10.001

Háden, G. P., Honing, H., Török, M., & Winkler, I. (2015). Detecting the temporal structure of sound sequences in newborn infants. *International Journal of Psychophysiology*. https://doi.org/10.1016/j.ijpsycho.2015.02.024

Haegens, S., & Zion Golumbic, E. (2018). Rhythmic facilitation of sensory processing: A critical review. *Neuroscience and Biobehavioral Reviews*, *86*(December 2017), 150–165. https://doi.org/10.1016/j.neubiorev.2017.12.002

Jones, M. R. (1976). Time, our lost dimension: Toward a new theory of perception, attention, and memory. *Psychological Review*, *83*(5), 323–355. https://doi.org/10.1037/0033-295X.83.5.323

Koelsch, S., Vuust, P., & Friston, K. (2019). Predictive Processes and the Peculiar Case of

Music. In *Trends in Cognitive Sciences*. https://doi.org/10.1016/j.tics.2018.10.006

Lakatos, P., Karmos, G., Mehta, A. D., Ulbert, I., & Schroeder, C. E. (2008). Entrainment of neuronal oscillations as a mechanism of attentional selection. *Science*. https://doi.org/10.1126/science.1154735

Large, E. W., & Jones, M. R. (1999). The dynamics of attending: How people track time-varying events. *Psychological Review*, *106*(1), 119–159. https://doi.org/10.1037//0033-295x.106.1.119

Merchant, H., & Bartolo, R. (2018). Primate beta oscillations and rhythmic behaviors. In *Journal of Neural Transmission* (Vol. 125, Issue 3, pp. 461–470). Springer-Verlag Wien. https://doi.org/10.1007/s00702-017-1716-9

Merchant, H., Grahn, J., Trainor, L., Rohrmeier, M., & Fitch, W. T. (2015). Finding the beat: A neural perspective across humans and non-human primates. *Philosophical Transactions of the Royal Society B: Biological Sciences*. https://doi.org/10.1098/rstb.2014.0093

Merker, B. H., Madison, G. S., & Eckerdal, P. (2009). On the role and origin of isochrony in human rhythmic entrainment. *Cortex*. https://doi.org/10.1016/j.cortex.2008.06.011

Morillon, B., Schroeder, C. E., Wyart, V., & Arnal, L. H. (2016). Temporal prediction in lieu of periodic stimulation. *Journal of Neuroscience*. https://doi.org/10.1523/JNEUROSCI.0836-15.2016

Mormann, F., Fell, J., Axmacher, N., Weber, B., Lehnertz, K., Elger, C. E., & Fernández, G. (2005). Phase/amplitude reset and theta-gamma interaction in the human medial temporal lobe during a continuous word recognition memory task. *Hippocampus*, *15*(7), 890–900. https://doi.org/10.1002/hipo.20117

Nobre, A.C., Rohenkohl, G., & Stokes, M. (2012). Nervous Anticipation : Top-Down Biasing across Space and Time. *Cognitive Neuroscience of Attention*.

Nobre, Anna C., & Van Ede, F. (2018). Anticipated moments: Temporal structure in attention. *Nature Reviews Neuroscience*, *19*(1), 34–48. https://doi.org/10.1038/nrn.2017.141

Nozaradan, S. (2014). Exploring how musical rhythm entrains brain activity with electroencephalogram frequency-tagging. In *Philosophical Transactions of the Royal Society B: Biological Sciences*. https://doi.org/10.1098/rstb.2013.0393

Nozaradan, S., Peretz, I., & Keller, P. E. (2016). Individual differences in rhythmic cortical entrainment correlate with predictive behavior in sensorimotor synchronization. *Scientific*

Reports. https://doi.org/10.1038/srep20612

Nozaradan, S., Peretz, I., Missal, M., & Mouraux, A. (2011). Tagging the Neuronal Entrainment to Beat and Meter. *Journal of Neuroscience*, *31*(28), 10234–10240. https://doi.org/10.1523/JNEUROSCI.0411-11.2011

Nozaradan, S., Schwartze, M., Obermeier, C., & Kotz, S. A. (2017a). Specific contributions of basal ganglia and cerebellum to the neural tracking of rhythm. *Cortex*, *95*, 156–168. https://doi.org/10.1016/j.cortex.2017.08.015

Nozaradan, S., Schwartze, M., Obermeier, C., & Kotz, S. A. (2017b). Specific contributions of basal ganglia and cerebellum to the neural tracking of rhythm. *Cortex*. https://doi.org/10.1016/j.cortex.2017.08.015

Nozaradan, S., Zerouali, Y., Peretz, I., & Mouraux, A. (2015). Capturing with EEG the Neural Entrainment and Coupling Underlying Sensorimotor Synchronization to the Beat. *Cerebral Cortex*, *25*(3), 736–747. https://doi.org/10.1093/cercor/bht261

Obleser, J., Herrmann, B., & Henry, M. J. (2012a). Neural oscillations in speech: Don't be enslaved by the envelope. *Frontiers in Human Neuroscience*. https://doi.org/10.3389/fnhum.2012.00250

Obleser, J., Herrmann, B., & Henry, M. J. (2012b). Neural Oscillations in Speech: Don't be Enslaved by the Envelope. *Frontiers in Human Neuroscience*, *0*(AUGUST), 250. https://doi.org/10.3389/FNHUM.2012.00250

Patel, A. D., & Iversen, J. R. (2014). The evolutionary neuroscience of musical beat perception: The Action Simulation for Auditory Prediction (ASAP) hypothesis. *Frontiers in Systems Neuroscience*. https://doi.org/10.3389/fnsys.2014.00057

Poudrier, È. (2020). The Influence of Rate and Accentuation on Subjective Rhythmization. *Music Perception*, *38*(1), 27–45. https://doi.org/10.1525/mp.2020.38.1.27

Sams, M., Paavilainen, P., Alho, K., & Näätänen, R. (1985). Auditory frequency discrimination and event-related potentials. *Electroencephalography and Clinical Neurophysiology/Evoked Potentials Section*, *62*(6), 437–448. https://doi.org/10.1016/0168-5597(85)90054-1

Schmidt-Kassow, M., Rothermich, K., Schwartze, M., & Kotz, S. A. (2011). Did you get the beat? Late proficient French-German learners extract strong–weak patterns in tonal but not in linguistic sequences. *NeuroImage*, *54*(1), 568–576. https://doi.org/10.1016/j.neuroimage.2010.07.062

Schroeder, C. E., & Lakatos, P. (2009). Low-frequency neuronal oscillations as instruments of sensory selection. *Trends in Neurosciences*, *32*(1), 9–18. https://doi.org/10.1016/j.tins.2008.09.012

Schröger, E., Giard, M. H., & Wolff, C. (2000). Auditory distraction: event-related potential and behavioral indices. *Clinical Neurophysiology*, *111*(8), 1450–1460. https://doi.org/10.1016/S1388-2457(00)00337-0

Schröger, E., Kotz, S. A., & SanMiguel, I. (2015). Bridging prediction and attention in current research on perception and action. *Brain Research*, *1626*, 1–13. https://doi.org/10.1016/j.brainres.2015.08.037

Schwartze, M., Keller, P. E., & Kotz, S. A. (2016). Spontaneous, synchronized, and corrective timing behavior in cerebellar lesion patients. *Behavioural Brain Research*, *312*, 285–293. https://doi.org/10.1016/j.bbr.2016.06.040

Schwartze, M., Rothermich, K., Schmidt-Kassow, M., & Kotz, S. A. (2011). Temporal regularity effects on pre-attentive and attentive processing of deviance. *Biological Psychology*, *87*(1), 146–151. https://doi.org/10.1016/j.biopsycho.2011.02.021

Schwartze, M., Stockert, A., & Kotz, S. A. (2015). Striatal contributions to sensory timing: Voxel-based lesion mapping of electrophysiological markers. *Cortex*, *71*, 332–340. https://doi.org/10.1016/j.cortex.2015.07.016

Shalev, N., Nobre, K., & van Ede, F. (2019). *Time for What: Breaking Down Temporal Anticipation*.

Thut, G., Miniussi, C., & Gross, J. (2012a). The functional importance of rhythmic activity in the brain. In *Current Biology* (Vol. 22, Issue 16). https://doi.org/10.1016/j.cub.2012.06.061

Thut, G., Miniussi, C., & Gross, J. (2012b). The functional importance of rhythmic activity in the brain. *Current Biology*, *22*(16), R658–R663. https://doi.org/10.1016/j.cub.2012.06.061

Waschke, L., Kloosterman, N. A., Obleser, J., & Garrett, D. D. (2021). Behavior needs neural variability. *Neuron*, *109*(5), 751–766. https://doi.org/10.1016/J.NEURON.2021.01.023

Zoefel, B., ten Oever, S., & Sack, A. T. (2018). The involvement of endogenous neural oscillations in the processing of rhythmic input: More than a regular repetition of evoked neural responses. *Frontiers in Neuroscience*, *12*(MAR), 1–13. https://doi.org/10.3389/fnins.2018.00095

Zoefel, B., & VanRullen, R. (2016). EEG oscillations entrain their phase to high-level features of

speech sound. *NeuroImage*, *124*, 16–23. https://doi.org/10.1016/j.neuroimage.2015.08.054

Supplementary materials

	Phase-angles Pre-DEV Vs Random			***Phase-angles Pre-DEV Vs post-DEV***			***MVL Pre-DEV Vs Random***		
	P vals	**Obs Diff**	**Eff Size**	**P vals**	**Obs Diff**	**Eff Size**	**P vals**	**Obs Diff**	**Eff Size**
Subj1	0.233	1.733	1.277	0.057	-2.715	-2.039	0.001	0.145	0.726
Subj2	0.689	0.719	0.520	0.906	0.073	0.056	0.001	0.121	0.654
Subj3	0.505	0.917	0.671	0.336	0.694	0.523	0.001	0.110	0.593
Subj4	0.461	-0.727	-0.539	0.755	0.160	0.121	0.001	0.156	0.834
Subj5	0.261	-1.629	-1.195	0.740	-0.176	-0.136	0.001	0.197	1.099
Subj6	0.479	0.598	0.446	0.692	0.169	0.132	0.001	0.138	0.729
Subj7	0.805	0.230	0.171	0.859	-0.089	-0.068	0.001	0.085	0.469
Subj8	0.662	-1.060	-0.758	0.069	-2.956	-2.141	0.001	0.096	0.479
Subj9	0.358	1.818	1.315	0.149	2.448	1.776	0.001	0.113	0.607
Subj10	0.606	-0.756	-0.551	0.719	-0.259	-0.196	0.001	0.109	0.616
Subj11	0.802	-0.360	-0.262	0.919	-0.100	-0.075	0.001	0.124	0.655
Subj12	0.656	0.800	0.581	0.953	0.069	0.051	0.001	0.115	0.646
Subj13	0.057	2.993	2.170	0.059	2.962	2.151	0.001	0.089	0.474
Subj14	0.094	2.838	2.048	0.146	2.633	1.900	0.001	0.141	0.721
Subj15	0.093	-2.489	-1.836	0.582	0.236	0.186	0.001	0.107	0.556
Subj16	0.123	-2.647	-1.911	0.905	0.155	0.112	0.001	0.135	0.704
Subj17	0.583	-1.229	-0.881	0.973	0.056	0.040	0.001	0.110	0.605
Subj18	0.402	1.909	1.358	0.034	-3.076	-2.205	0.001	0.135	0.718
Subj19	0.778	-0.704	-0.504	0.339	1.127	0.839	0.001	0.122	0.643
Subj20	0.314	1.407	1.033	0.475	-0.559	-0.416	0.001	0.174	0.918

Suppl. Table 1 – Circular statistics for phase-angles and mean vector lengths
Statistical testing of the phase-angle differences between neural activity at the stimulation frequency (1.5Hz) for, in order, STD tones pre-DEV versus a random distribution and pre-DEV versus post-DEV. On the right, the statistical comparison of trial-based mean vector lengths (MVL) for STD tones pre-DEV versus a random distribution. The phase-angles are extracted, per tone, in the pre-stimulus intervals in a time-window of 60ms (1/1.5Hz/10) and averaged with circular mean statistics. The MVL are calculated based on the trial-level phase-angle circular means. Statistical testing was performed, independently, by means of 1000 permutation tests. In the table are provided, in order the p-values (rounded to 3 decimals), observed differences and effect sizes per subject.

	Binary %	Triplet %	Combined %	Other %
Subj1	19,3	26	9,4	45,3
Subj2	20,8	18,2	18,2	42,8
Subj3	20,3	22,9	16,1	40,7
Subj4	20,3	29,2	12,5	38
Subj5	22,4	21,4	17,7	38,5
Subj6	17,2	19,3	13	50,5
Subj7	18,2	26	12,5	43,3
Subj8	26	21,4	9,4	43,2
Subj9	17,2	20,8	14,1	47,9
Subj10	15,1	26,6	12	46,3
Subj11	22,4	17,7	13,5	46,4
Subj12	25	21,4	14,6	39
Subj13	17,7	20,8	15,6	45,9
Subj14	24	20,8	17,2	38
Subj15	17,2	20,8	19,8	42,2
Subj16	21,9	27,6	9,9	40,6
Subj17	22,9	18,8	10,9	47,4
Subj18	25	22,9	12,5	39,6
Subj19	19,8	16,7	12,5	51
Subj20	18,8	20,8	12	48,4

Table 2 – Grouping preferences from the beat modelling.
The table reports the percentages of individual preferences for (in order) binary, triplet, combined (binary + triplet) beat. The last column includes all trials which could not be classified as the above-mentioned beat strategies.